

# Quasi-Elastic Neutrino-Nucleus Reactions

M. VALVERDE, J. NIEVES AND J.E. AMARO

*Departamento de Física Moderna, Universidad de Granada, E-18071 Granada, Spain*

The quasi-elastic contribution of the nuclear inclusive electron scattering model developed in A. Gil, J. Nieves, and E. Oset: Nucl. Phys. A **627** (1997) 543; is extended to the study of electroweak Charged Current (CC) induced nuclear reactions at intermediate energies of interest for future neutrino oscillation experiments. The model accounts for long range nuclear (RPA) correlations, Final State Interaction and Coulomb corrections. RPA correlations are shown to play a crucial role in the whole range of neutrino energies, up to 500 MeV, studied in this work. Predictions for inclusive muon capture for different nuclei, and for the reactions  $^{12}\text{C}(\nu_\mu, \mu^-)X$  and  $^{12}\text{C}(\nu_e, e^-)X$  near threshold are also given.

*PACS:* 25.30.Pt, 13.15.+g

*Key words:* Quasi-elastic neutrino-nucleus reactions, Nuclear RPA effects.

## 1 Introduction

There are two main reasons that motivate the study of neutrino scattering off nuclei. Firstly the topic is of interest by itself because of the interest of knowing how the nuclear medium affects the nucleon axial current. The other main reason is that projected neutrino experiments require of a good control over systematic errors coming from the uncertainty in the neutrino-nucleus cross section. This second issue has motivated big efforts in this topic at low (few MeV) and intermediate nuclear excitations energies (a few hundred MeV).

Any model aiming at describing the interaction of neutrinos with nuclei should be firstly tested against the existing data on the interaction of real and virtual photons with nuclei. The model developed in [1] (inclusive electro-nuclear reactions) and [2] (inclusive photo-nuclear reactions) has been successfully compared with data at intermediate energies (nuclear excitation energies ranging from about 100 MeV to 500 or 600 MeV). The building blocks of this model are: i) a gauge invariant model for the interaction of real and virtual photons with nucleons, mesons and nucleon resonances with parameters determined from the vacuum data, and ii) a microscopic treatment of nuclear effects, including long and short range nuclear correlations [3], Final State Interactions (FSI), explicit meson and  $\Delta(1232)$  degrees of freedom, two and three nucleon absorption channels, etc. Nuclear effects are computed starting from a Local Fermi Gas picture of the nucleus, which is an accurate approximation to deal with inclusive processes which explore the whole nuclear volume, see [2] and [4]. The parameters of the model are completely fixed from previous hadron-nucleus studies: pionic atoms, elastic and inelastic pion-nucleus reactions,  $\Lambda$ -hypernuclei, etc. [5]. The gauge boson (real and virtual photons and charged bosons  $W^\pm$ ) coupling constants are also determined in the vacuum. Thus the model of [1] and [2] has no free parameters, and hence these results are predictions deduced from the nuclear microscopic framework developed in [3] and [5]. In

this talk, we show an extension of the nuclear inclusive quasi-elastic (QE) electron scattering model of [1], including the axial CC current, to describe neutrino and antineutrino induced nuclear reactions in the QE region. We will not show here many details of the model, for a detailed discussion we refer the reader to [6]. For an extension to neutral currents see [7], where nucleon knock-out reactions are also studied.

## 2 INCLUSIVE CROSS SECTION

We will expose here the general formalism focusing on the neutrino CC reaction. The generalization to antineutrino CC reactions or muon capture is straightforward. In the laboratory frame, the differential cross section for the process  $\nu_l(k) + A_Z \rightarrow$

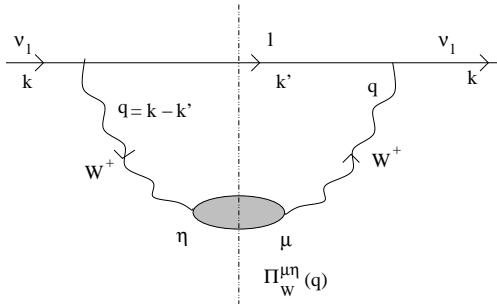


Fig. 1. Diagrammatic representation of the neutrino selfenergy in nuclear matter.

$l^-(k') + X$  reads:

$$\frac{d^2\sigma}{d\Omega(\hat{k}')dE_l'} = \frac{|\mathbf{k}'|}{|\mathbf{k}|} \frac{G^2}{4\pi^2} L_{\mu\sigma} W^{\mu\sigma} \quad (1)$$

with  $L$  and  $W$  the leptonic and hadronic tensors, respectively. On the other hand, the inclusive CC nuclear cross section is related to the imaginary part of the neutrino self-energy (see Fig. 1) in the medium by:

$$\sigma = -\frac{1}{|\mathbf{k}|} \int d^3\mathbf{r} \text{Im}\Sigma_\nu(k; \rho(r)) \quad (2)$$

We get  $\text{Im}\Sigma_\nu$  by following the prescription of the Cutkosky's rules: in this case we cut with a vertical straight line (see Fig. 1) the intermediate lepton state and those implied by the  $W$ -boson polarization. Those states are placed on shell by taking the imaginary part of the propagator, self-energy, etc. We obtain for  $k^0 > 0$

$$\text{Im}\Sigma_\nu(k) = \frac{8G\Theta(q^0)}{\sqrt{2}M_W^2} \int \frac{d^3\mathbf{k}'}{(2\pi)^3} \frac{\text{Im}\{\Pi_W^{\mu\eta} L_{\eta\mu}\}}{2E_l'} \quad (3)$$

and thus, the hadronic tensor is basically an integral over the nuclear volume of the  $W$ -selfenergy ( $\Pi_W^{\mu\nu}(q; \rho)$ ) inside the nuclear medium. We can then take into account the in-medium effects (such as  $W$ -absorption by pairs of nucleons, pion production, delta resonances,...) by including the correspondent diagram in the shaded loop of Fig. 1. Further details can be found in Ref. [6].

### 3 QE CONTRIBUTION TO $\Pi_W^{\mu\nu}(q; \rho)$

The virtual  $W^+$  can be absorbed by one nucleon (neutron) leading to the QE peak of the nuclear response function. Such a contribution corresponds to a 1p1h nuclear excitation. At sufficiently high energies other channels (such as pion production, two nucleon absorption, etc. ) open and should be taken into account. We consider a structure of the  $V - A$  type for the  $W^+pn$  vertex, and use PCAC and invariance under G-parity to relate the pseudoscalar form factor to the axial one and to discard a term of the form  $(p^\mu + p'^\mu)\gamma_5$  in the axial sector, respectively. Invariance under time reversal guarantees that all form factors are real. Besides, and thanks to isospin symmetry, the vector form factors are related to the electromagnetic ones. We find

$$W^{\mu\nu}(q) = \frac{\cos^2 \theta_C}{2M^2} \int_0^\infty dr r^2 \Theta(q^0) \int \frac{d^3 \mathbf{p}}{4\pi^2} \frac{M}{E(\mathbf{p})} \frac{M}{E(\mathbf{p} + \mathbf{q})} \Theta(k_F^n(r) - |\mathbf{p}|) \Theta(|\mathbf{p} + \mathbf{q}| - k_F^p(r)) \delta(q^0 + E(\mathbf{p} + \mathbf{q}) - E(\mathbf{p})) A^{\nu\mu}(p, q)|_{p^0=E(\mathbf{p})} \quad (4)$$

with the local Fermi momentum  $k_F(r) = (3\pi^2 \rho(r)/2)^{1/3}$ ,  $M$  the nucleon mass, and  $E(\mathbf{p}) = \sqrt{M^2 + \mathbf{p}^2}$ . We will work on a non-symmetric nuclear matter with different Fermi sea levels for protons,  $k_F^p$ , than for neutrons,  $k_F^n$  (equation above, but replacing  $\rho/2$  by  $\rho_p$  or  $\rho_n$ , with  $\rho = \rho_p + \rho_n$ ). Finally,  $A^{\mu\nu}$  is the CC nucleon tensor [6]. The  $d^3 \mathbf{p}$  integrations above can be done analytically and all of them are determined by the imaginary part of isospin asymmetric Lindhard function,  $\bar{U}(q, k_F^n, k_F^p)$ . Explicit expressions can be found in [6].

We take into account polarization effects by substituting the particle-hole (1p1h) response by an RPA response consisting in a series of ph and  $\Delta$ -hole excitations as shown in Fig. 2. We use an effective Landau-Migdal ph-ph interaction [8]:  $V = c_0 \{f_0 + f'_0 \boldsymbol{\tau}_1 \boldsymbol{\tau}_2 + g_0 \boldsymbol{\sigma}_1 \boldsymbol{\sigma}_2 + g'_0 \boldsymbol{\sigma}_1 \boldsymbol{\sigma}_2 \boldsymbol{\tau}_1 \boldsymbol{\tau}_2\}$ , where only the isovector terms contribute to CC processes. In the  $S = 1 = T$  channel ( $\boldsymbol{\sigma} \boldsymbol{\sigma} \boldsymbol{\tau} \boldsymbol{\tau}$  operator) we use an interaction [1, 2, 5] with explicit  $\pi$  (longitudinal) and  $\rho$  (transverse) exchanges. The  $\Delta(1232)$  degrees of freedom are also included in the  $S = 1 = T$  channel of the RPA response. This effective interaction is non-relativistic, and then for consistency we will neglect terms of order  $\mathcal{O}(p^2/M^2)$  when summing up the RPA series.

We ensure the correct energy balance, of both neutrino and antineutrino CC induced process in finite nuclei, by modifying the energy conserving  $\delta$  function in Eq. (4) to account for the  $Q$ -value of the reaction.

We also consider the effect of the Coulomb field of the nucleus acting on the ejected charged lepton. This is done by including the lepton self-energy  $\Sigma_C = 2k'^0 V_C(r)$  in the intermediate lepton propagator of Fig. 1.

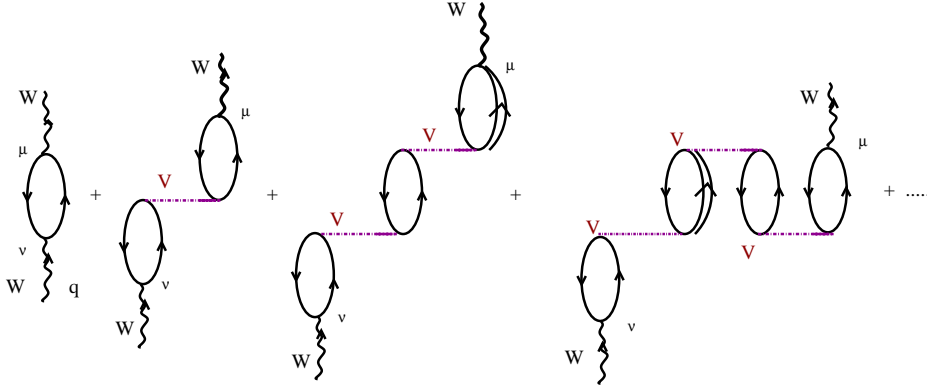


Fig. 2. Set of irreducible diagrams responsible for the polarization (RPA) effects in the 1p1h contribution to the  $W$ -selfenergy.

Finally, we account for the FSI by using nucleon propagators properly dressed with a realistic self-energy in the medium, which depends explicitly on the energy and the momentum [9]. Thus, we rewrite the imaginary part of the Lindhard function (ph propagator) in terms of particle and hole spectral functions  $S_{p,h}(\omega, \mathbf{p}; \rho)$ .

#### 4 RESULTS

We present in Fig. 3 and Table 1 our theoretical predictions and a comparison of those to the experimental measurements of the inclusive  $^{12}\text{C}(\nu_\mu, \mu^-)X$  and  $^{12}\text{C}(\nu_e, e^-)X$  reactions near threshold. Pauli blocking and the use of the correct energy balance improve the results, but only once RPA and Coulomb effects are included a good description of data is achieved.

Table 1. Experimental and theoretical flux averaged  $^{12}\text{C}(\nu_\mu, \mu^-)X$  and  $^{12}\text{C}(\nu_e, e^-)X$  cross sections in  $10^{-40} \text{ cm}^2$  units. We label our predictions as in Fig. 3.

	RPA	Exp [10] and [11]		
$\bar{\sigma}(\nu_\mu, \mu^-)$	11.9	LSND'95 $8.3 \pm 0.7 \pm 1.6$	LSND'97 $11.2 \pm 0.3 \pm 1.8$	LSND'02 $10.6 \pm 0.3 \pm 1.8$
$\bar{\sigma}(\nu_e, e^-)$	0.14	KARMEN $0.15 \pm 0.01 \pm 0.01$	LSND $0.15 \pm 0.01 \pm 0.01$	LAMPF $0.141 \pm 0.023$

Given the success in describing the LSND measurement of the reaction  $^{12}\text{C}(\nu_\mu, \mu^-)X$  near threshold, it seems natural to further test our model by studying

the closely related process of the inclusive muon capture in  $^{12}\text{C}$ . Furthermore, and since there is abundant and accurate measurements on nuclear inclusive muon capture rates through the whole Periodic Table, we have also calculated muon capture widths for a few selected nuclei. Results are compiled in Table 2. Data are quite accurate, with precisions smaller than 1%, quite far from the theoretical uncertainties of any existing model. Medium polarization effects (RPA correlations), once more, are essential to describe the data. Despite of the huge range of variation of the capture widths (note,  $\Gamma^{\text{exp}}$  varies from about  $4 \times 10^4 \text{ s}^{-1}$  in  $^{12}\text{C}$  to  $1300 \times 10^4 \text{ s}^{-1}$  in  $^{208}\text{Pb}$ ), the agreement to data is quite good for all studied nuclei, with discrepancies of about 15% at most. It is precisely for  $^{12}\text{C}$ , where we find the greatest discrepancy with experiment. Nevertheless, our model provides one of the best existing combined description of the inclusive muon capture in  $^{12}\text{C}$  and the LSND measurement of the reaction  $^{12}\text{C} (\nu_{\mu}, \mu^{-})X$  near threshold.

Table 2. Experimental and theoretical total muon capture widths for different nuclei. Experimental data are taken from Ref. [12], and when more than one measurement is quoted in [12], we use a weighted average:  $\bar{\Gamma}/\sigma^2 = \frac{\sum_i \Gamma_i/\sigma_i^2}{\sum_i 1/\sigma_i^2}$ . We quote two different theoretical results: i) Pauli+ $\bar{Q}$  obtained without including FSI effects and RPA correlations ; ii) the full calculation, including all nuclear effects with the exception of FSI, and denoted as RPA. In the last column we show the relative discrepancies existing between the theoretical predictions given in the third column and data.

	Pauli+ $\bar{Q}$ [ $10^4 \text{ s}^{-1}$ ]	RPA [ $10^4 \text{ s}^{-1}$ ]	Exp [ $10^4 \text{ s}^{-1}$ ]	$(\Gamma^{\text{Exp}} - \Gamma^{\text{Th}}) / \Gamma^{\text{Exp}}$
$^{12}\text{C}$	5.42	3.21	$3.78 \pm 0.03$	0.15
$^{16}\text{O}$	17.56	10.41	$10.24 \pm 0.06$	-0.02
$^{18}\text{O}$	11.94	7.77	$8.80 \pm 0.15$	0.12
$^{23}\text{Na}$	58.38	35.03	$37.73 \pm 0.14$	0.07
$^{40}\text{Ca}$	465.5	257.9	$252.5 \pm 0.6$	-0.02
$^{44}\text{Ca}$	318	189	$179 \pm 4$	-0.06
$^{75}\text{As}$	1148	679	$609 \pm 4$	-0.11
$^{112}\text{Cd}$	1825	1078	$1061 \pm 9$	-0.02
$^{208}\text{Pb}$	1939	1310	$1311 \pm 8$	0.00

At intermediate energies the predictions of our model become reliable not only for integrated cross sections, but also for differential cross sections. We present results for incoming neutrino energies within the interval 150–400 (250–500) MeV for electron (muon) species. In Figs. 4 and 5, FSI effects on differential cross section are shown. As expected, FSI provides a broadening and a significant reduction of the strength of the QE peak. Nevertheless the integrated cross section is only slightly modified. In Table 3 we compile electron neutrino and antineutrino inclusive QE integrated cross sections from oxygen. Though FSI change importantly the differential cross sections, it plays a minor role when one considers total cross sections. When medium polarization effects are not considered, FSI provides significant reductions

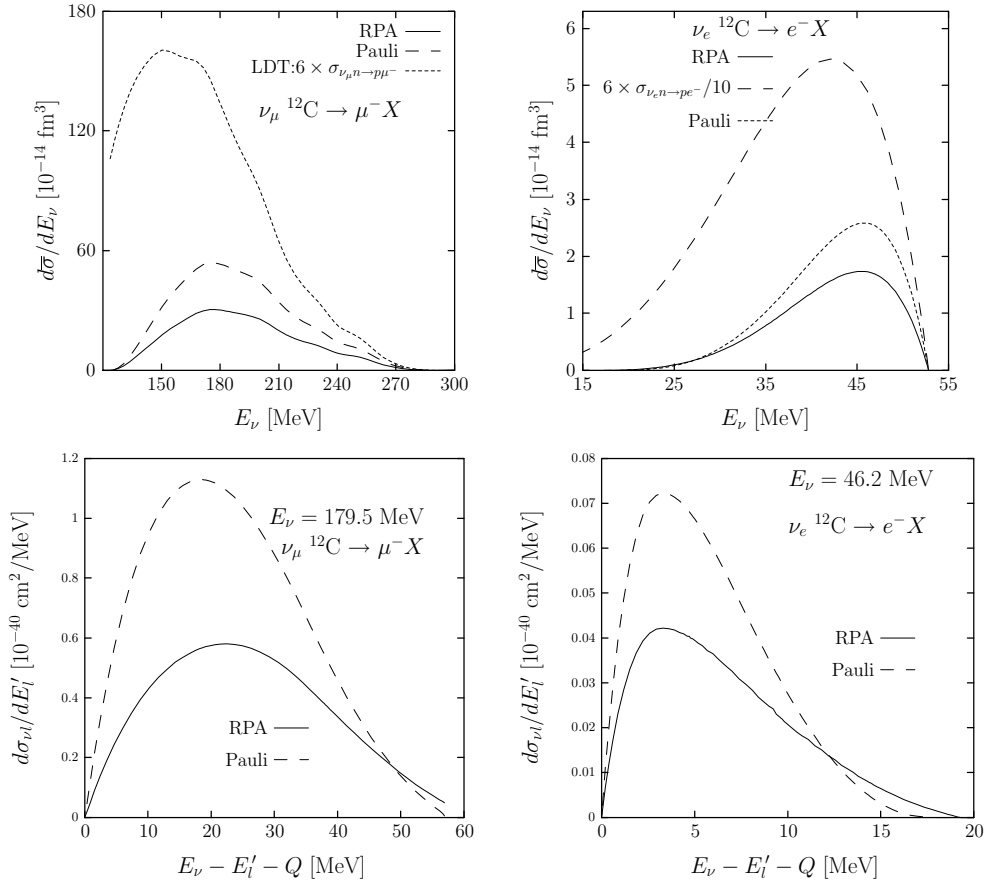


Fig. 3. Theoretical predictions for the  $^{12}\text{C} (\nu_\mu, \mu^-)X$  and the  $^{12}\text{C} (\nu_e, e^-)X$  reactions near threshold. In addition to the full calculation (denoted as RPA), with all nuclear effects with the exception of the FSI ones, we show results obtained without including RPA, FSI and Coulomb corrections (denoted as Pauli), and also results (denoted as LDT) obtained by multiplying the free space cross section by the number of neutrons of  $^{12}\text{C}$ .

(15–30%) of the cross sections. However, when RPA corrections are included the reductions becomes more moderate, always smaller than 7%, and even there exist some cases where FSI enhances the cross sections. This can be easily understood by looking at Fig. 5. There, we see that FSI increases the cross section for high energy transfer. But for nuclear excitation energies higher than those around the QE peak, the RPA corrections are certainly less important than in the peak region. Hence, the RPA suppression of the FSI distribution is significantly smaller than the RPA reduction of the distribution determined by the ordinary Lindhard function.

### Quasi-Elastic Neutrino-Nucleus Reactions

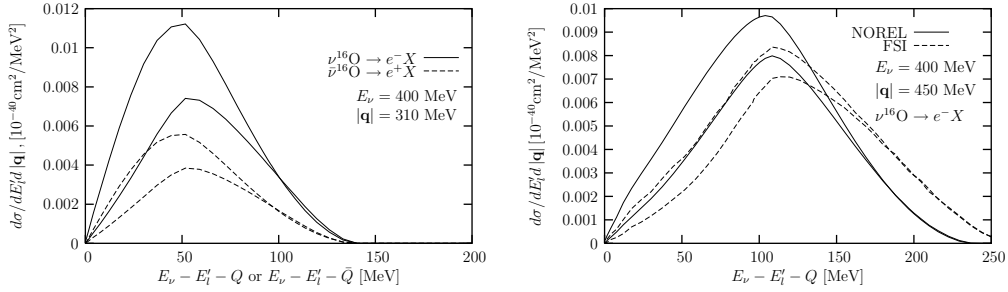


Fig. 4. Inclusive QE double differential cross sections in oxygen as a function of the transferred energy, for two values (310 and 450 MeV) of the transferred momentum. The incoming neutrino (antineutrino) energy is 400 MeV. We show results non-relativistic nucleon kinematics and with (FSI) and without (NOREL) FSI effects. For all cases, we show the effect of taking into account RPA correlations and Coulomb corrections (lower lines at the peak).

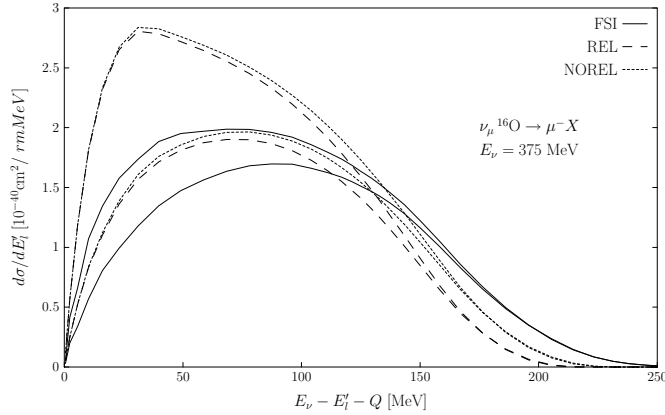


Fig. 5. Muon neutrino inclusive QE differential cross sections in oxygen as a function of the transferred energy. The incoming neutrino energy is 375 MeV. The notation for the theoretical predictions is the same as in Fig. 4.

### References

- [1] A. Gil, J. Nieves, and E. Oset: Nucl. Phys. A **627** (1997) 543; *ibidem*: Nucl. Phys. A **627** (1997) 598.
- [2] R.C. Carrasco and E. Oset: Nucl. Phys. A **536** (1992) 445; R.C. Carrasco, E. Oset, and L.L. Salcedo: Nucl. Phys. A **541** (1992) 585; R.C. Carrasco, M.J. Vicente-Vacas, and E. Oset: Nucl. Phys. A **570** (1994) 701.

Table 3. Electron neutrino (left) and antineutrino (right) inclusive QE integrated cross sections from oxygen. We present results for relativistic ('REL') and non-relativistic nucleon kinematics. In this latter case, we present results with ('FSI') and without ('NOREL') FSI effects. Results, denoted as 'RPA' and 'Pauli', have been obtained with and without including RPA correlations and Coulomb corrections, respectively.

$E_\nu$ [MeV]		$\sigma(^{16}\text{O}(\nu_e, e^-)X) 10^{-40} \text{cm}^2$			$\sigma(^{16}\text{O}(\bar{\nu}_e, e^+)X) 10^{-40} \text{cm}^2$		
		REL	NOREL	FSI	REL	NOREL	FSI
400	Pauli	389.4	416.6	352.5	130.0	139.1	121.0
	RPA	294.7	322.6	303.6	91.9	101.9	104.8
310	Pauli	281.4	297.4	240.6	98.1	104.0	87.2
	RPA	192.2	209.0	195.2	65.9	72.4	73.0
220	Pauli	149.5	156.2	121.2	60.7	63.6	51.0
	RPA	90.1	97.3	92.8	36.8	40.0	40.2

- [3] E. Oset, H. Toki, and W. Weise: Phys. Rep. 83 (1982) 281.
- [4] J.E. Amaro, C. Maieron, J. Nieves, and M. Valverde: Eur. Phys. Jour. A **24** (2005) 343; Erratum Eur. Phys. Jour. A **24** (2005) 307;
- [5] J. Nieves, E. Oset, and C. García-Recio: Nucl. Phys. A **554** (1993) 509; *ibidem*: Nucl. Phys. A **554** (1993) 554; J. Nieves and E. Oset: Phys. Rev. C **47** (1993) 1478. E. Oset, et al.: Prog. Theor. Phys. Suppl. 117 (1994) 461; C. Albertus, J.E. Amaro, and J. Nieves: Phys. Rev. Lett. 89 (2002) 032501; *ibidem*: Phys. Rev. C **67** (2003) 034604.
- [6] J. Nieves, J.E. Amaro, and M. Valverde: Phys. Rev. C **70** (2004) 055503; Erratum Phys. Rev. C **72** (2005) 019902.
- [7] J. Nieves, M. Valverde, and M. Vicente-Vacas: Phys. Rev. C, in print. hep-ph/0511204.
- [8] J. Speth, E. Werner, and W. Wild: Phys. Rep. 33 (1977) 127; J. Speth, V. Klemt, J. Wambach, and G.E. Brown: Nucl. Phys. A **343** (1980) 382.
- [9] P. Fernández de Córdoba, and E. Oset: Phys. Rev. C **46** (1992) 1697.
- [10] M. Albert, et al.: Phys. Rev. C **51** (1995) R1065; C. Athanassopoulos, et al.: Phys. Rev. C **56** (1997) 2806; L.B. Auerbach, et al.: Phys. Rev. C **66** (2002) 015501.
- [11] B. Zeitnitz: Prog. Part. Nucl. Phys. 32 (1994) 351; B.E. Bodmann et al.: Phys. Lett. B **332** (1994) 251; C. Athanassopoulos, et al.: Phys. Rev. C **55** (1997) 2078; D.A. Krakauer et al.: Phys. Rev. C **45** (1992) 2450.
- [12] T. Suzuki, D.F. Measday, and J.P. Roalsvig: Phys. Rev. C **35** (1987) 2212.